Supporting Information

Predicted novel two-dimensional ferromagnetic VO_2 with high Curie temperature and ferroelasticity

Wen-Zhi Xiao [a] *, Ying-Xue Feng [a],

[a] School of Computational Science and Electronics, Hunan Institute of Engineering, Xiangtan 411104,China

The search process of the evolutionary algorithm:

The Evolutionary Algorithm within the Universal Structure Predictor: Evolutionary Xtallography (USPEX) software is used to determine the global minimum energy configuration of VO_2 binary compounds with 3-12 atoms in each unit cell and a 1:2 element ratio. The population iteration includes an initial population size of 90, subsequent generations with a population size of 40, a total of 40 generations, and retention of the top 50% energy individuals from each generation to produce offspring. In addition, 50% of the population is generated by inheritance during the evolutionary process. We re-optimized the good structures from USPEX to determinate the energy order of the structures. To avoid omissions, we performed the USPEX procedure twice.

The orientation dependent Young's modulus Y(θ) and Poisson's ratio ν(θ):

The orientation dependent Young's modulus Y(θ) and Poisson's ratio ν(θ) can be calculated from the following equations:

$$\begin{cases} Y(\theta) = \dfrac{Y_{zz}}{\cos^4\theta + d_2 \sin^2\theta\cos^2\theta + d_3 \sin^4\theta} \\ \nu(\theta) = \dfrac{\nu_{zz}\cos^4\theta - d_1 \sin^2\theta\cos^2\theta + \nu_{zz}\sin^4\theta}{\cos^4\theta + d_2 \sin^2\theta\cos^2\theta + d_3 \sin^4\theta} \end{cases} \quad (5)$$

where d_1, d_2, d_3, Y_{zz}, and ν_{zz} are variables related to the elastic constants described in detail in the references [1, 2, 3].

*Corresponding author: xiaowenzhi@hnie.edu.cn

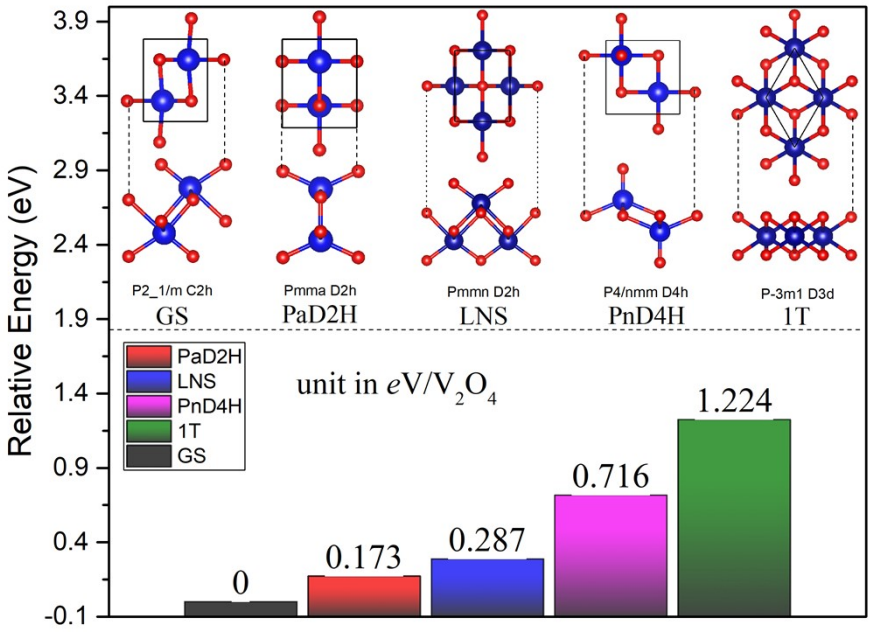

Figure S1. Calculated relative energies with respect to the GS-VO_2 in their FM ground states. The inset shows the corresponding top and side views of different configurations. All calculations were performed at the DFT+U level for different structures in the FM order.

Table S1. Optimized structural properties of the four different 2D VO_2 crystal structures. ***a***, ***b*** and ***c*** are the lattice constants. Atomic positions are the Wyckoff positions for each independent atom in fractional coordinates. All the parameters are calculated by the GGA+U method in the ferromagnetic order for all the structures.

Structure	GS	PaD2H	LSN	PnD4H	1T
Space group	P2_1/m (#11)	Pmma (#51)	Pmmn (#59)	P4/nmm (#129)	P-3m1 (#164)
Point group	5 [C2h]	8 [D2h]	8 [D2h]	15 [D4h]	20 [D3d]
a (Å)	2.963	3.281	2.959	3.759	2.197
b (Å)	3.824	3.915	3.886	3.759	2.197
c (Å)	20.0	20.0	20.0	20.0	20.0
Positions	O(0.746;1/4;0.394)	O(0.0;1/4;0.411)	O(1/2;0.0;0.474)	O(1/2;1/2;1/2)	O(1/3;2/3;0.450)
	O(0.747;1/4;0.525)	O(1/2;1/4;0.536)	O(1/2;0.0;0.602)	O(0.0;1/2;0.381)	
	V(0.700;3/4;0.552)	V(1/2;3/4,0.553)	V(0.0;0.0;0.551)	V(0.0;1/2;0.460)	V(0.0;0.0;0.500)

Table S2. The summrized values of lattice constant ***a/b*** (Å), band gaps (eV), exchange coupling parameters J_i (meV), and T_C (K) obtained from GGA+U scheme with vaious effective $U_{eff} = \bar{U} \quad J$.

U_{eff}	***a/b***	E_g	J_1	J_2	J_3	J_4	T_C
0.0	2.963/3.724	0.000	106.41	55.33	-3.75	36.44	
1.0	2.956/3.786	0.363	74.21	21.45	-3.12	14.06	
2.0	2.962/3.806	0.960	55.92	18.73	0.07	12.22	
3.0	2.965/3.827	1.500	45.93	16.76	1.06	10.91	1070
4.0	2.969/3.848	1.956	39.54	15.40	1.29	10.68	970
5.0	2.974/3.868	2.358	34.95	14.34	1.53	9.98	900
6.0	2.980/3.888	2.613	31.34	13.38	1.65	9.76	825

Table S3. The summrized values of total magnetic moment (MM), exchange coupling parameters J_i , and T_C obtained from GGA+U scheme for VO_2 monolayer without and with strain at 5%.

Stain (%)	MM (μ_B)	J_1 (meV)	J_2 (meV)	J_3 (meV)	J_4 (meV)	T_C (K)
0.00	2.00	45.83	16.81	1.08	10.98	1066
5.00	2.00	36.96	19.14	-2.50	7.11	895

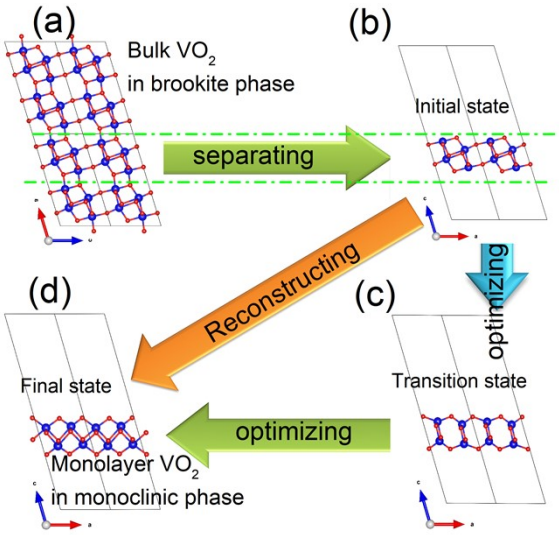

Figure S2. Schematic representation of the formation process of a stable VO_2 monolayer [4]: To break the V-O bonds along the (100) plane of (a) bulk VO_2 in the brookite phase and then to form the (b) initial monolayer, passing through (c) a series of intermediate states to reach (d) a final restructured monolayer of VO_2 in the monoclinic phase.

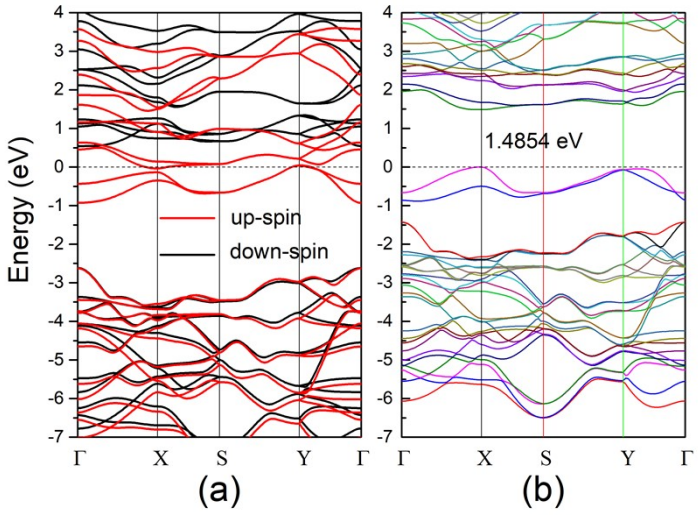

Figure S3. Electronic band structures of VO_2 monolayer obtained at (a) GGA and (b) GGA+U+SOC levels. The Fermi level is indicated by a dashed line at 0.0 eV. The electronic band structures do not change significantly with respect to those obtained at the GGA+U level.

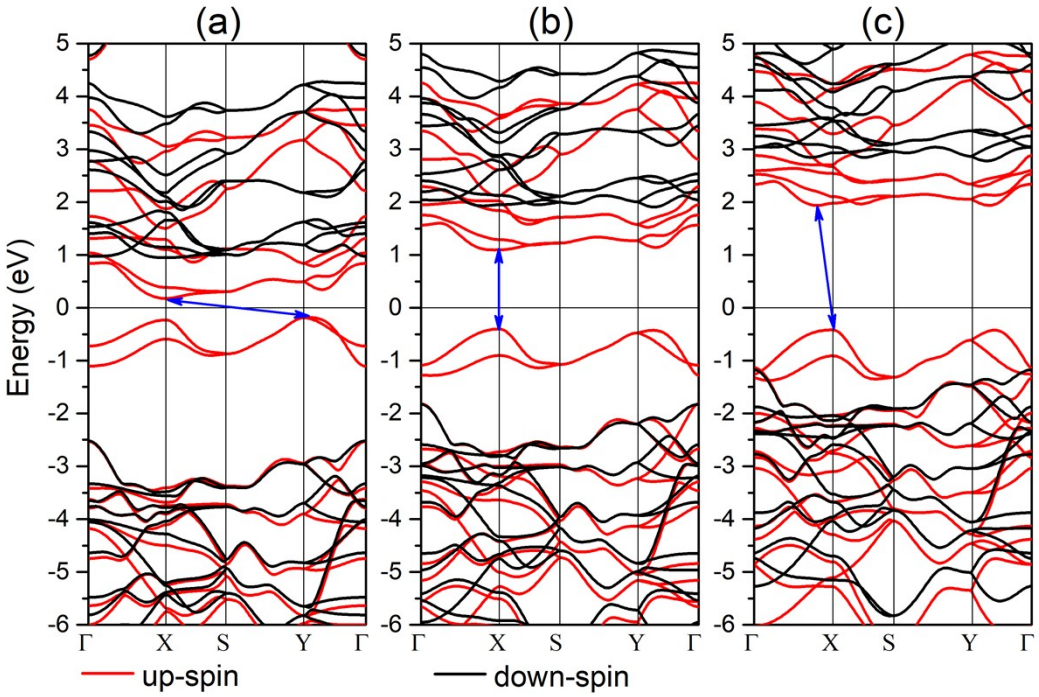

Figure S4. Electronic band structures of VO_2 monolayer obtained at GGA+U level with effective U_{eff} of (a) 1.0, 3.0 (b), and (c) 5.0 eV.

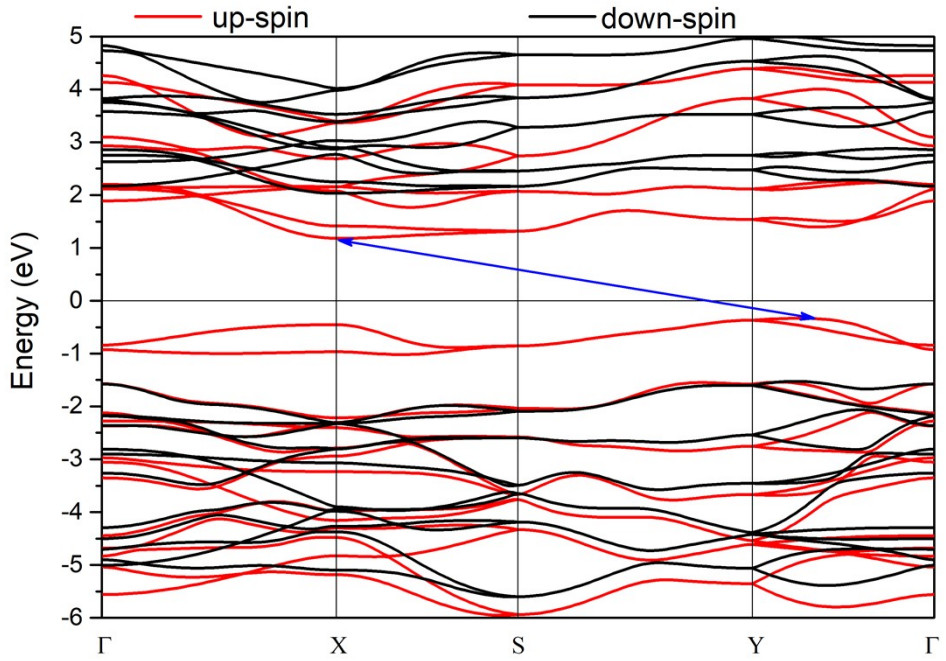

Figure S5. Electronic band structures of VO_2 monolayer obtained from GGA+U scheme under strain of 5%.

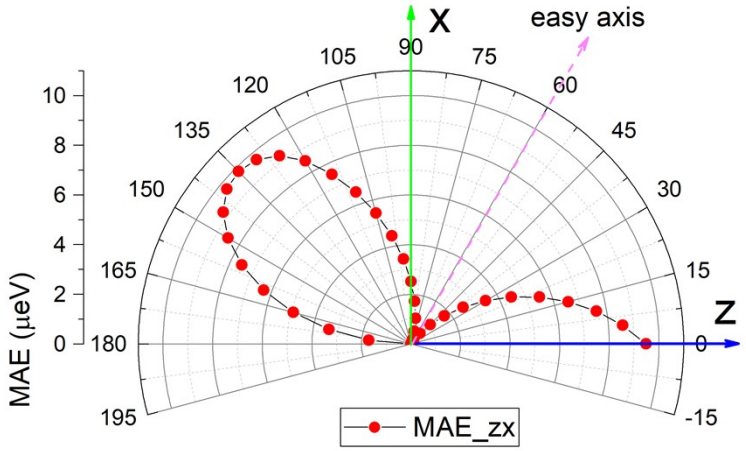

Figure S6. Projected angle dependent magnetic anisotropic energy in the ZX plane, with respect to the global minimum energy.

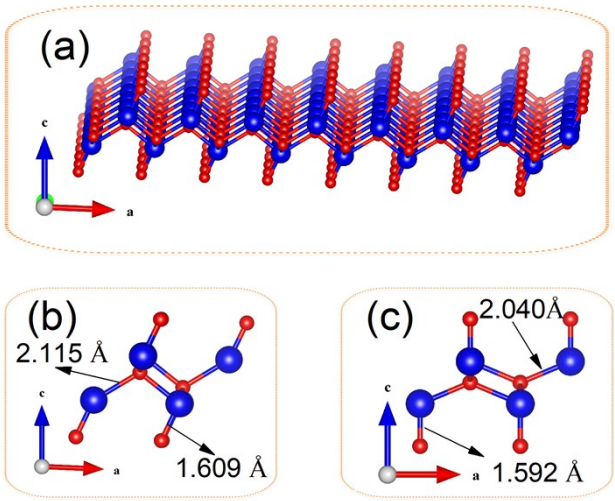

Figure S7. (a) Side view and (b) top view of the atomic structure of the seventh image in the path of the NEB. (a) Side view of the atomic structure of the paraelastic phase in the path of the NEB. The paraelastic phase has a P4/nmm symmetry, which has been verified to be stable [5]. The maximum and minimum bond lengths are labelled for comparison. The small difference in the bond lengths implies no structure breaking.

[1] L. Wang, A. Kutana, X. Zou and B. I. Yakobson, Electro-mechanical anisotropy of phosphorene. *Nanoscale*, 2015, **7**, 9746–9751.

[2] H. Wang, X. Li, P. Li, J. Yang, δ-Phosphorene: a two dimensional material with a highly negative Poisson's ratio. *Nanoscale*, 2017, **9**(2), 850-855.

[3] E. Cadelano, P. L. Palla, S. Giordano, L. Colombo, Elastic properties of hydrogenated grapheme. *Phys. Rev. B*, 2010, **82**(23), 235414.

[4] Y. Zhou, P. Yan, S. Zhang, C. Ma, T. Ge, X. Zheng, L. Zhang,J. Jiang, Y. Shen, J. Chen, Q. Xu, Conversion of non-van der Waals VO_2 solid to 2D ferromagnet by CO_2-induced phase engineering. *Nano Today*, 2021, **40**, 101272.

[5] Z. K. Tang, X. B. Li, D. Y. Zhang, Y. N. Zhang, L. M. Liu, Two-dimensional square-pyramidal VO_2 with tunable electronic properties. *J. Mater. Chem. C*, 2015, **3**(13), 3189-3197.